JOURNAL OF
EMERGING INVESTIGATORS

Article

Visualizing black holes and wormholes through raytracing

Neer Mehta[1], Bart Ripperda[2]

[1] The International School of Bangalore, Bangalore, Karnataka, India

[2] Canadian Institute for Theoretical Astrophysics, University of Toronto, Toronto, Ontario, Canada

SUMMARY

We explored the visualization of black holes and wormholes using code and ray-tracing programs. We introduced an advancement in astrophysics with the creation of a 4-color screen of a traversable Morris-Thorne wormhole, achieved through the utilization of flexible object-oriented ray tracer (FOORT), a ray-tracing software. Our research gives insight into the detection of black holes and wormholes in deep space; the 4-color screens are reflective of the gravitational lensing that occurs according to the laws of general relativity. We hypothesized that a Schwarzschild black hole would have a similar 4-color screen to a Morris-Thorne wormhole because neither object has angular momentum. In order to demonstrate the effect of angular momentum on gravitational lensing, we also explored Kerr black holes, since the nature of most cosmic objects gives them a spin. For wormholes, only a stationary, non-rotating, 2-way traversable wormhole was considered. Our hypothesis was supported by observing the similarity between the 4-color panels of the Schwarzschild black hole and a Morris-Thorne wormhole. We also examined the difference between the panels by constructing a subtracted image which highlighted the contrasts. This research sheds light on the difference between the gravitational properties of a Morris-Thorne wormhole, a Schwarzschild black hole, and a Kerr black hole. We concluded that the use of a 4-color screen can help grasp what black holes and wormholes do to photon particles in their locality, and how they would appear through instruments such as the Hubble Telescope in outer space.

INTRODUCTION

In the realm of human inquiry, it remains difficult to truly grasp what one cannot see. Light, therefore, is one of the crucial media through which the universe is perceived. While the scientific community continues to understand and research the nature of light, light can be used to detect what cannot be seen directly. A relevant example in astrophysics are black holes. Black holes form from the inward collapse of large stars, with cores heavier than three solar masses, due to the force of gravity (1). This implosion causes the matter of the star to be compactified into an infinitely dense point in space known as a singularity, though it should be noted that not all black holes' formation follows this pathway (2).

Black holes can be described by three parameters: mass, spin, and charge. Mass defines the gravitational potential of an object; the singularity that has an extremely large mass, therefore, has an extremely strong gravitational field (3). The force of gravity is strong enough that light cannot escape, making observations of black holes a considerable challenge. The spin on a black hole would define the shape of the black hole, since frame dragging acts when massive bodies have an angular momentum (4). The charge would define a black hole's interaction with matter; however, it is still unclear whether a charged black hole would exist given its ability to attract particles to achieve neutrality (5). The focus of this research paper is on spin and mass.

The first detection of a black hole occurred in an X-ray binary system, Cygnus X-1, through orbital mechanics and X-ray emissions (6). X-ray binary systems consist of two celestial objects orbiting around their center of mass and emitting significant amounts of X-rays. A previous study showed that it was a binary system of a visible blue supergiant star and an "invisible" black hole (7).

One approach to visualizing black holes is through telescopes. In the image of the black hole at the center of the Messier 87 galaxy, taken by the Event Horizon Telescope, there is a disc of matter that emits light surrounding it, known as an accretion disk (8). This is formed by diffuse matter that orbits the central object at high angular moments while slowly losing energy and spiraling inward. Due to friction and gravity, the matter is compressed, and the temperature is raised. This causes electromagnetic radiation to be emitted, which results in a glowing yellow and orange disc seen around the center of black holes (9).

Another method to understand the detection of massive objects is gravitational lensing along with ray tracing, which is described below. Gravitational lensing studies the effects of light deflection on the appearance of cosmic objects. Massive objects in space warp the 3+1 space and time dimensions. Gravitational lensing has been researched in astrophysics to infer the presence of cosmic phenomena (10). It has been used to discover a dwarf galaxy that was invisible to telescopes (11). If a black hole were to be placed between the Earth and a distant light source, the light source would appear distorted due to the gravitational field of the black hole warping the space-time fabric. The event horizon of a black hole is a boundary beyond which not even light can escape the gravitational pull. Light rays that pass close to the spherical event horizon of the black hole, whose radius is known as the Schwarzschild radius, get deflected, and their path becomes bent (12). The distant light source seems to be warped. A Schwarzschild black hole is a special black hole that has a radius equal to the Schwarzschild radius, has no charge, no angular momentum, and is the simplest form of a black hole that we are researching in this manuscript. Schwarzschild blackholes also have space-time symmetry, meaning their

https://doi.org/10.59720/24-074

gravitational field is spherically symmetrical (13).

Nonetheless, black holes are not the only phenomenon predicted by Einstein's General Theory of Relativity, there are mathematical metrics for wormholes too. Wormholes are hypothetical tunnels in space-time that could connect distant regions of the universe. There are different wormholes categorized based on whether they are traversable and whether they are one-way or two-way (14). A commonly studied wormhole is the Morris-Thorne wormhole, which is a two-way traversable wormhole (15). This means that objects can enter and exit from both sides.

Studies have shown that mathematically, the gravitational lensing around Schwarzschild black holes is similar to the gravitational lensing around Morris-Thorne wormholes (16). The similarities are derived from the fact that they are both spherically symmetrical and static (no angular momentum) (17). One common modeling technique is ray tracing, a computational approach that simulates the paths of light bending around massive bodies by advancing rays over short distances and using local derivatives to calculate new directions (18). In this research, we use ray tracing and gravitational lensing around cosmic bodies to explore these similarities. If wormholes exist, analyzing these screens could help locate them through their lensing signatures. Additionally, improving gravitational lensing techniques enhances our ability to interpret astronomical observations, which is crucial for black hole imaging and wormhole detection.

The phenomenon of gravitational lensing can also produce optical effects that can help us analyze properties of black holes. For example, light rays can complete an entire orbit around a black hole, known as an Einstein ring, and using this data, quantities such as the mass and properties of the black hole can be determined (19). In addition, the study conducted by Tsukamoto discusses the similarity between the Einstein rings found around Schwarzschild black holes and wormholes (20). This research aimed to explore the similarities between Schwarzschild blank holes and Morris-Thorne wormholes by generating 4-color screens which use ray-tracing and gravitational lensing around cosmic bodies.
A method of viewing ray tracing of gravitationally lensed photons (photons are particles that represent a quantum of light) is to render a theoretical figure of where the rays would appear to the observer, which can be achieved with a 4-color screen. The color is based on the quadrant where they originated. 4-color screens have been used in research efforts for simulation purposes and understanding the properties of particles around black holes (21). It is a powerful tool to visualize the mysteries of our universe. Another method that has been used in studies is the General relativitY Orbit Tracer of Observatoire de Paris (GYOTO), which also employs ray-tracing techniques (22). GYOTO uses radiative processes, such as absorption, emission, and scattering, to match observational data. For studies, like the present one, mainly focused just on ray tracing of non-charged cosmic bodies, these features seemed to add unnecessary bulk.

Additionally, the 4-color screen was chosen for this research because it fits with the research aim. Our research aimed to analyze the similarity of the gravitational fields around black holes and wormholes, and the 4-color screen is a better fit as its output is a 2D screen which has the same pixel size as other screens generated, thus images can be manipulated easily (such as subtracting them). The four colors also make it simple to gauge which quadrant the rays begin from, and they stand out in contrast to the remainder of the image.

We hypothesized that a Schwarzschild black hole would have a similar 4-color screen to a Morris-Thorne wormhole. We believe this is true because both objects are predictions of Einstein's theory of general relativity. This hypothesis was made based on the mathematical study reviewed earlier (16, 17). We created 4-color screens for black holes and wormholes using C++, metrics, and raytracing. To compare the 4-color screens, we used a Python code to subtract the pixels of the images, and we analysed the differences between a Schwarzschild black hole and a Morris-Thorne wormhole. The 4-color screens showed a great degree of symmetry; however, they also brought light to the differences in gravitational lensing around the event horizon of the black hole and the throat of the wormhole. Our work, thus, mitigates a gap in the existing literature regarding the usage of 4-color screens to create wormholes, specifically its direct application to distinguishing between black holes and wormholes. It also supplements the existing work that relies heavily on numerical solutions with a visual representation, using numerical code.

RESULTS

A geodesic is a path followed by objects that are only acted upon by the force of gravity. In general relativity, they represent the straightest possible paths in curved space-time (23). We developed a Python script to construct a three-dimensional visualization of how the gravitational field of black holes and wormholes can influence the path of photons or geodesics. We also used the flexible object-oriented ray tracer (FOORT) to create a color-coded two-dimensional image. FOORT is a raytracing software in C++ developed by Dr. Daniel Mayerson and Dr. Fabio Bacchini (24).

We coded the Morris-Thorne wormhole metric in FOORT to calculate the position of geodesics on an imaginary coordinate grid (**Figure 1**)**.** The photons were color-coded based on which coordinate they originated from. The 4-color screen of the wormhole has a center black circle, which depicts the throat (**Figure 1a**). The throat of a wormhole is the narrow tunnel that connects the two openings. There is a band of gravitational lensing in the form of rings around the throat. There is also a larger band where the colors differ from the original color of that quadrant, which again shows gravitational lensing. A zoomed-in wormhole was also created for comparison purposes (**Figure 1b**).

The 4-color screen of the Schwarzschild black hole shows a black circle, the event horizon, and colors to represent the quadrant of the photons (**Figure 2**). A Schwarzschild black hole is the simplest black hole, that has no rotation and has no charge (25). The Schwarzschild radius is the radius of the sphere in which an object of mass *M* needs to be compressed in order to turn into a black hole.

The 4-color screen of a black hole and a wormhole look similar. For a more fine-grained comparison of the two 4-color screens, we zoomed into the wormhole to equate the radius of both figures, superimposed the figures, and subtracted the pixels Morris-Thorne wormhole from the Schwarzschild black hole. The subtracted figure considers the absolute value of the difference between pixels at the same coordinate in the two original figures (**Figure 3**). The subtracted figure had three distinct visible rings around the horizon, which suggests

https://doi.org/10.59720/24-074

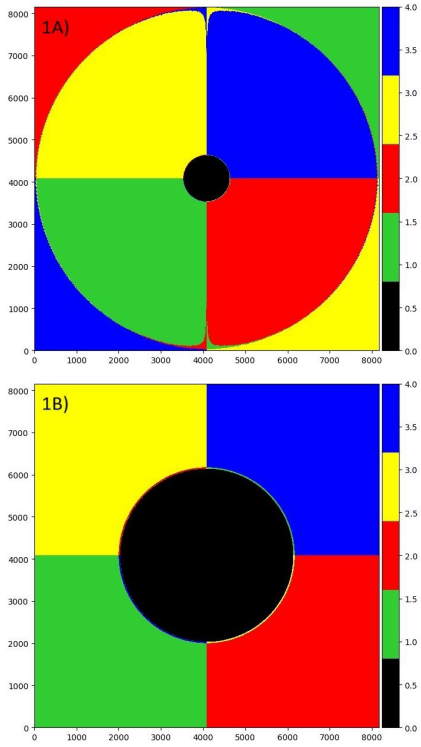

Figure 1: Simulated Morris-Thorne wormhole with throat size of 1 M. Generated through FOORT. The scale on the x and y axes is logarithmic for all 4-color screens and depicts pixel count, so regardless of the scale of zoom, the number of pixels generated are the same. The color bar shows the value assigned to each pixel color. A black pixel would represent the throat of wormhole or event horizon for black holes, green originated in quadrant 1, red originated in quadrant 2, blue originated in quadant 3, and yellow originated in quadrant 4. The colors on this 4-color screen do not match the quadrants I stated above due to the gravitational lensing, which is proof of the warping effect. **A)** Simulated Morris-Thorne wormhole with a screen size of 15. The mesh used was square subdivision, with 65,536 initial pixels, 10,000 iteration pixels, a maximum of 6 subdivisions, and 150,000 total maximum pixels. **B)** Morris-Thorne wormhole with the same values except for a screen size of 4. This figure is the same as **A,** except it is zoomed in for comparison purposes.

that gravitational lensing for the black hole covered a larger distance than that for the wormhole. Additionally, new colors, e.g., light blue, emerged in the subtracted figure. This is visible in the outermost bands of the rings around the event horizon. This suggests different extents of gravitational lensing.

The above observations support our hypothesis that Morris-Thorne wormhole and a Schwarzschild black hole would have similar 4-color screens partly because they do not have angular momentum. To demonstrate the effect of angular momentum on the gravitational field of an object, we included the 4-color screen of a black hole with angular momentum. Black holes with angular momenta are known as Kerr black holes. A Kerr black hole—one with an angular momentum of 0.9 *M*—has a warping effect (26). This is observed from the 4-color screen generated through FOORT (**Figure 4**). The event horizon is no longer a perfect circle, and the rings around the event horizon form a thicker band. The gravitational lensing of the Kerr black hole with a spin of 0.9 *M* is visibly greater than the gravitational lensing by a

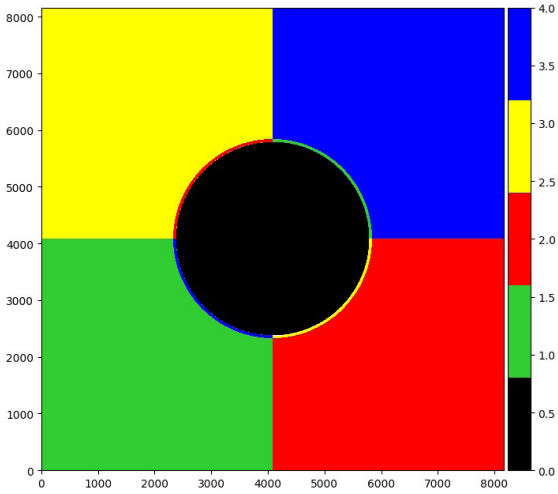

Figure 2: Simulated Schwarzschild black hole. Generated through FOORT. The screen size was set to 12. The mesh used was square subdivision, with 65,536 initial pixels, 10,000 iteration pixels, a maximum of 6 subdivisions, and 150,000 total maximum pixels.

Schwarzschild black hole with a spin of 0.0 *M* and the Morris-Thorne wormhole. Warping effect, the result of a gravitational field bending the fabric of space-time, increases with angular momentum, as described by Howard (26). The thicker band and greater distortion of the event horizon are evidence of frame dragging due to angular momentum.

Shifting the focus back to wormholes, a three-dimensional visual depiction of a wormhole with a throat size of 1 *M* was simulated (**Figure 5**). The path of a light ray in red has been plotted. The cosmic tunnel allows objects to pass through and exit through the opposite end. This shows how light is bent in the wormhole. The same effect is reflected in the 4-color screen of the wormhole with a large circle that has flipped colors from the rest of the background.

It is also helpful to refer to the flat-space metric in this case (**Figure 6**). A flat space metric is one that does not possess any gravitational field. Green originates in the first quadrant but appears in the third quadrant in the wormhole image. This is the region of gravitational lensing for the wormhole.

For a depiction of gravitational lensing in 3 dimensions, the black hole space-time in spatial dimensions is graphed (**Figure 7a**). The axes have mass units. The event horizon is depicted as a red sphere with a radius of 2 *M* units. A light ray travelling in the vicinity of this black hole is influenced by its gravitational field and can follow different orbits depending on the initial conditions of the particle. As examples, we simulated five conditions (**Figure 7b-e**). In the first scenario, rays can be trapped in the event horizon of the black hole. For instance, the light ray with initial position (8, π/2, 0) and velocity of c = 1 ends up colliding with the black hole directly (**Figure 7b**). Secondly, in some cases, light could complete an entire orbit and return to the source (**Figure 7c**). The complete orbit and return are known as the primary Einstein ring of a Schwarzschild black hole, investigated by Müller (27). In the example shown, the initial position of the photon was (20, π/2, 0) in the direction of a clockwise rotation of 0.2535 radians from the x-axis. Tunning the direction to 0.2490 radians clockwise from the x axis resulted in a photon that completes 2 orbits before returning to the source (**Figure**

https://doi.org/10.59720/24-074

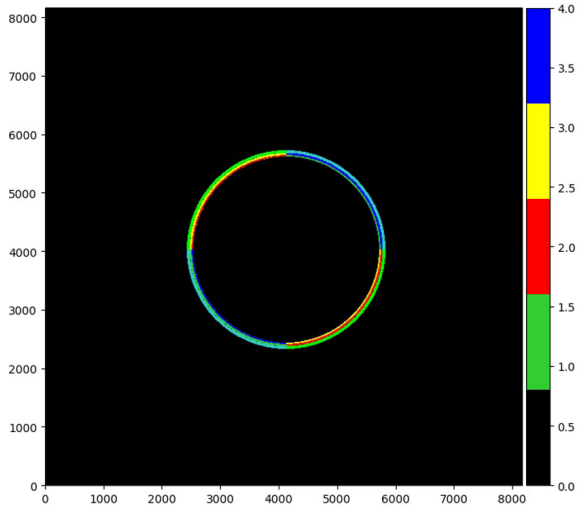

Figure 3: Subtraction of the 4-colours of the wormhole from the image of a Schwarzschild black hole. Generated through a Python script. Using the Python software and cv2.abdiff function, all overlapping portions of the black hole and wormhole were subtracted, and at places where colors were different, the average was calculated. For example, where the same color overlaps, we get black pixels. When the colors are different, we get a different colored pixel, such as the light blue arc-shaped band, which is generated when green and blue pixels overlap.

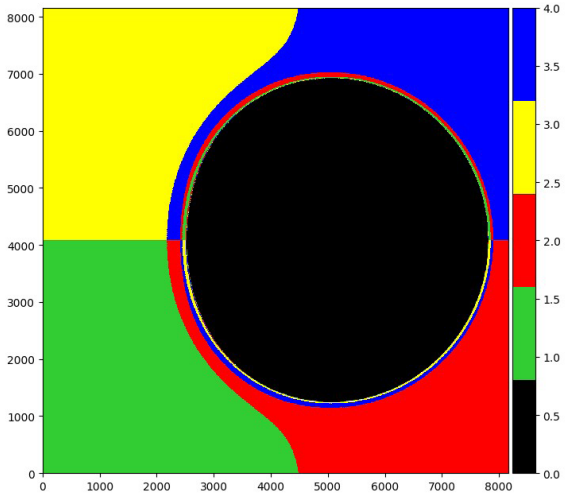

Figure 4: Kerr black hole with angular momentum of 0.9 M. Generated through FOORT. The screen size was set to 15. The mesh used was square subdivision, with 65,536 initial pixels, 10,000 iteration pixels, a maximum of 6 subdivisions, and 150,000 total maximum pixels.

7e). This is known as the secondary Einstein ring, which has been investigated by Müller too (27). Furthermore, the light may enter an infinite orbit around the black hole. This is referred to as the homoclinic orbit (**Figure 7d**). This occurs under the conditions when the particle begins at (20, π/2, -10) and has an initial angle of precisely:

$$\sin^{-1}\left(\sqrt{\frac{27}{4}\times\left(\frac{2M}{20}\right)^2\times\left(1-\frac{2M}{20}\right)}\right)$$

M = 1 so Θ is approximately 0.2490 radians. Lastly, in certain cases, the black hole could also cause gravitational lensing, resulting in warping of the light that reaches our eyes; (14, -π/2, π/4) light ray with initial position of (14, -π/2, π/4) (**Figure 7f**).

DISCUSSION

The subtracted figure is mostly black pixels, except for the three colored bands. This suggests that the majority of the black hole and wormhole 4-color screens were the same. This finding does align with our hypothesis that there would be similarities between the two 4-color screens. The similarity mainly stems from the fact that both the Schwarzschild black hole and the Morris-Thorne wormhole do not have angular momentum, and an equal gravitational pull is exerted on all sides. The difference, indicated by the colored bands, was in the region of gravitational lensing. This region that is just outside the event horizon for the Schwarzschild black hole is observably larger than the region just outside the throat of the Morris-Thorne wormhole. The similarities in gravitational lensing have been illustrated mathematically in a previous study, which is also explored in the present paper (16). The distinction arises because the photon sphere surrounding the Schwarzschild black hole extends further outwards compared to the region around a wormhole.

This 4-color screen-based investigation was further expanded to include black hole metrics with non-zero angular momentum. The Kerr black hole generated shows gravitational lensing to a much greater extent. This is because rotating masses cause the frame-dragging of spacetime in addition to the gravitational force of attraction of the black hole at rest. Our findings align with existing research conducted by Dubey and Sen on gravitational lensing and frame-dragging effects around rotating black holes (4). Their study highlights the frame-dragging effect that is caused by rotating bodies, particularly justifying the warping effect observed in the 4-color screens of Kerr black holes that were created to show that angular momentum has an effect on gravitational lensing. Our findings also replicate the research conducted by Staelens, in which the Kerr black holes generated had the same frame dragging effects on the 4-color screen as the ones generated in our manuscript, given that both papers used the FOORT for 4-color screen generation (21). Our manuscript, however, does not focus solely on black holes, but builds on FOORT by adding a metric to view wormholes. Since wormholes do not have an associated mass, their angular momentum can take arbitrarily large values. This paper does not consider the angular momentum wormhole metrics; the Kerr black hole was examined as it portrays the difference between a stationary and spinning mass, and we found a very warped event horizon for the Kerr black hole. This helped make the argument that a wormhole with angular momentum would have a different 4-color screen. However, it was challenging to code this metric, and the geodesics took extremely long to integrate given the massless nature of the wormhole, thus the spinning wormhole metric was not considered.

Incorporating the angular momentum in wormhole metrics is a promising area for future research. Including different wormhole metrics would create more detailed 4-color screens and comparisons. Expanding the program to use more colors to encode different light rays would create more visually rich and particularized images. Additionally, the code could

https://doi.org/10.59720/24-074

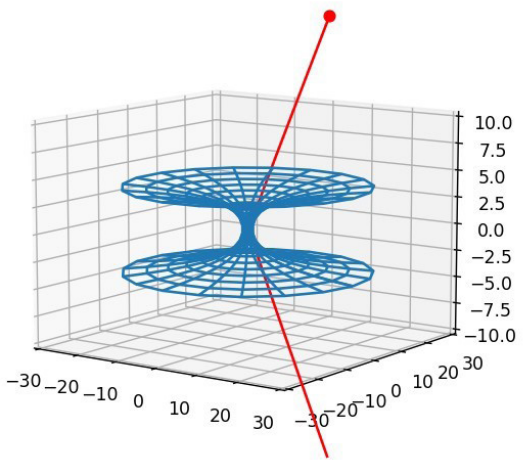

Figure 5: 3-Dimensional Morris-Thorne wormhole with b = 1 M. A single geodesic in red is marked. Units of the axes are all in arbitrary mass, with the throat size being 1 mass unit wide. This figure was coded in Python using the wormhole metric. The initial position was provided and used to calculate future positions and momenta using iteration loops with a Runge Kutta 4th order integrator. These values were put into arrays which were later referenced to track and mark the path of the geodesic.

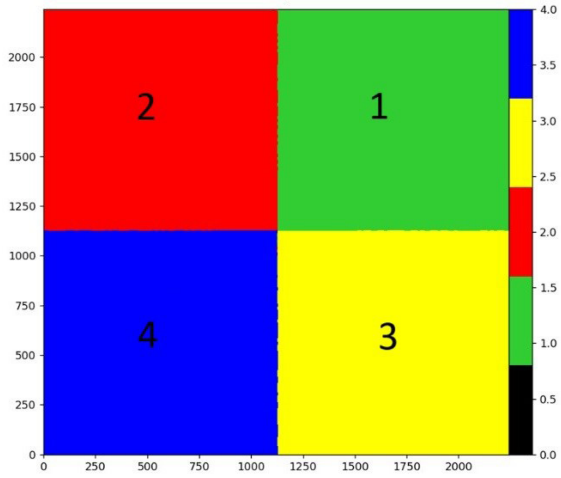

Figure 6: 4-color screen of flat space time. Generated through FOORT. The original color of geodesics is depicted depending on the quadrant they originate from. Geodesics that start in the first quadrant are given a value of 1, and whichever pixel the geodesic ends within will be green. Similarly, quadrant 2 has red geodesics with a value of 2, quadrant 3 has blue geodesics with a value of 4, and quadrant 4 has yellow geodesics with a value of 3. The screen size was set to 15, however the subdivision mesh did not work as the FOORT software did not have to divide the pixels more than once. There were 65,536 initial pixels, a single subdivision, and 10,000 iteration pixels. The axis labels are adjusted to account for the iteration stopping after one instead of 6 iterations.

also be further expanded to simulate the effect of warping on massive and charged particles, which would involve changing the geodesic equation and adding the Lorentz force (the electromagnetic force acting on charged particles) to the equations of motion in general relativity. Combining these additions, more comprehensive images could be generated. The codes for 3D black holes and wormholes were created for this paper, but we were only able to integrate singular geodesics.

In conclusion, when looking at a 4-color screen generated by the FOORT code, the thickness of the gravitational lensing rings that are directly around the horizon, the shape of the event horizon or throat, and the entire region of gravitational lensing should be considered. By analyzing the symmetry and thickness of gravitational lensing rings we observed similarities and differences between not only a black hole and a wormhole but also between stationary and rotating objects. The Schwarzschild black hole and Morris-Thorne wormhole had a similar symmetrical 4-color screen, with only different colored bands indicating different gravitational field strengths. The Kerr black hole had a 4-color screen with an asymmetrical center and gravitational lensing pattern. This tells us that angular momentum affects gravitational fields. Overall, a 4-color screen helps us get an introductory visualization on how light rays would be warped around black holes and wormholes.

MATERIALS AND METHODS

Defining parameter values and initial conditions for simulations

When calculating the path of light rays, we used 3D polar coordinates in the form of (r, θ, Φ), where r is the distance from the origin, θ is the colatitude angle, Φ is the azimuthal angle. The speed of light, c, was set equal to 1 for all calculations. This is often done in theoretical physics to simplify calculations in a consistent way and normalize velocities in terms of the speed of light. Similarly, the gravitational constant, G, was set equal to 1. This results in distances such as the Schwarzschild radius or throat size, being measured in the units of mass (M). The initial coordinates of a light particle are expressed in polar coordinates. The radius was set as r_i = 20 M. The initial momentum in polar coordinates is set as (u_r, $u\theta$, $u\Phi$), where $u\theta$ = 0, so the motion is bounded to the equatorial place. Other momenta components are defined as:

$$u_r = \frac{1}{\sqrt{-\left(1-\frac{2M}{20}\right)}} \times \cos(\alpha),\ u_\phi = 20M \times \sin(\alpha)$$

Here, α is the angle between the radial direction and the component of velocity.

Simulating a Schwarzschild black hole

A Schwarzschild black hole is described by the Schwarzschild metric (28):

$$ds^2 = -\left(1-\frac{r_s}{r}\right)dt^2 + \left(1-\frac{r_s}{r}\right)^{-1}dr^2 + r^2(d\theta^2 + \sin^2\theta\, d\phi^2) \qquad \text{(Eqn 1)}$$

Where ds^2 represents the spacetime interval between two points. The Schwarzschild radius (rs) is calculated with the formula $2GM/c^2 = 2M$.

To calculate geodesics with this metric, we defined $\alpha = \sqrt{(1-2M/r)}$ as the lapse vector, β = (0,0,0) as the shift vector, and γ as a matrix depiction of the Schwarzschild metric.

$$\gamma = \begin{bmatrix} -\left(1-\frac{2M}{r}\right) & 0 & 0 & 0 \\ 0 & \left(1-\frac{2M}{r}\right)^{-1} & 0 & 0 \\ 0 & 0 & r^2 & 0 \\ 0 & 0 & 0 & r^2\sin^2\theta \end{bmatrix} \qquad \text{(Eqn 2)}$$

https://doi.org/10.59720/24-074

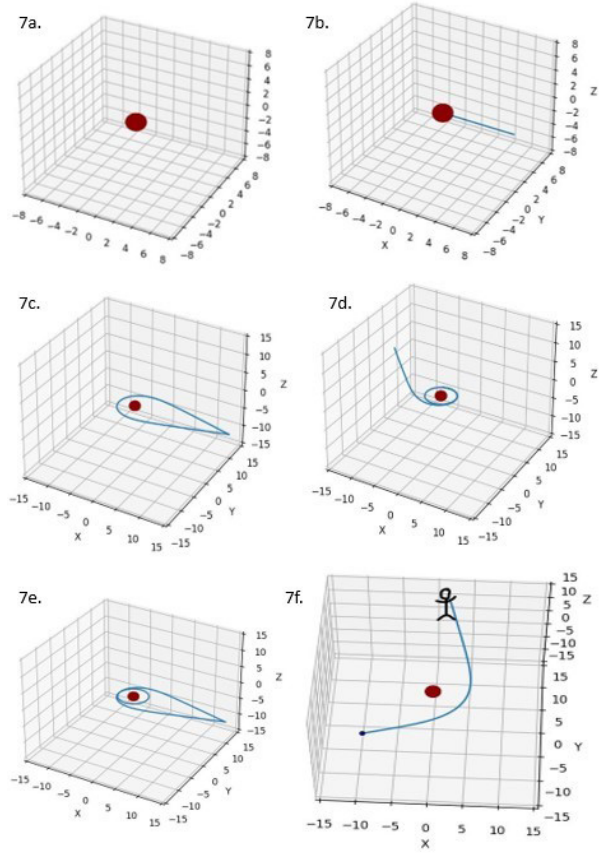

Figure 7: Event horizon of a black hole with radius of 2 M units and behavior of different photons approaching the event horizon. The red sphere is the event horizon. Behaviors of a single geodesic of one photon at the event horizon were generated using a Python script for different scenarios: **A)** A singular black hole with radius 2 M. **B)** A single photon particle entering the event horizon of the black hole. **C)** A photon completing a primary Einstein ring around the black hole. **D)** A photon completing a homoclinic orbit around the black hole. **E)** A photon completing a secondary Einstein ring around a black hole. **F)** Gravitational lensing of a photon around a black hole. From the perspective of the observer, the object is realistically on the right of the black hole. However, some light would be warped around the black hole and the object would also appear faintly to the left of the black hole.

Then, an initial position was provided to the photon, and its respective momentum and direction were calculated. The Runge-Kutta method of the 4th order was used to create an approximation of the geodesic path.

Simulating photon behavior

To be able to properly understand this phenomenon, a 2D screen that ray traces multiple geodesics can be created to get an idea of how a black hole would warp light.

Simulating a Kerr black hole

A Kerr black hole is described with a metric in Boyer-Lindquist coordinates (29):

$$ds^2 = -\left(1-\frac{r_S r}{\Sigma}\right)dt^2 + \frac{\Sigma}{\Delta}dr^2 + \sum d\theta^2 + \left(r^2 + a^2 + \frac{r_S r a^2}{\Sigma}\sin^2\theta\right)\sin^2\theta\, d\phi^2 - \frac{2r_S r a \sin^2\theta}{\Sigma}dt d\phi \quad \text{(Eqn 3)}$$

Here, a is the rescaled angular momentum, which equals J/M with J being the physical angular momentum; $r_s = 2M$ is the Schwarzschild radius of the black hole,

$$\sum = r^2 + a^2\cos^2\theta \quad \text{(Eqn 4)}$$

$$\Delta = r^2 - r_s r + a^2 \quad \text{(Eqn 5)}$$

The covariant elements of the Kerr Metric provide information about the geometry of space time and are in the matrix below:

$$g = \begin{bmatrix} -\left(1-\left(\frac{2r}{\Sigma}\right)\right) & 0 & 0 & -2ar\times\frac{\sin^2(\theta)}{\Sigma} \\ 0 & \frac{\Sigma}{\Delta} & 0 & 0 \\ 0 & 0 & \Sigma & 0 \\ -2ar\times\frac{\sin^2(\theta)}{\Sigma} & 0 & 0 & \frac{A}{\Sigma\times\sin^2(\theta)} \end{bmatrix} \quad \text{(Eqn 6)}$$

Here,

$$A = (r^2+a^2)^2 - \Delta\times a^2\times\sin^2(\theta) \quad \text{(Eqn 7)}$$

The contravariant elements are the inverse of this matrix.

The 4-color screen of the Kerr black hole is a spinning black hole with an angular momentum of $a = 0.9\,M$. The black hole is viewed from the equatorial plane, which means the observer is located at $\theta = \pi/2$.

Simulating a wormhole

Wormholes can be thought of as cosmic tunnels that connect two remote regions in the space-time manifold. Wormholes can be traversable or non-traversable and one-way or two-way. For this research, we utilized a traversable Morris-Thorne Wormhole. The metric for this wormhole is (30):

$$ds^2 = -dt^2 + dr^2 + (b^2+r^2)(d\theta^2 + sin^2\,\theta\, d\phi^2) \quad \text{(Eqn 8)}$$

The covariant elements of this metric are defined by:

$$g = \begin{bmatrix} -1 & 0 & 0 & 0 \\ 0 & 1 & 0 & 0 \\ 0 & 0 & b^2+r^2 & 0 \\ 0 & 0 & 0 & (b^2+r^2)\times\sin^2(\theta) \end{bmatrix} \quad \text{(Eqn 9)}$$

The contravariant elements are the inverse of the matrix.

The FOORT code was expanded in order to include the metric of a wormhole. A variable was created to represent the horizon, which is the throat size. The elements of the covariant and contravariant matrices were then referenced in a series of calculations. The metric only had elements in the diagonal (g[0][0], g[1][1], g[2][2], g[3][3] – representing the elements of the matrix in [row][column] form).

ACKNOWLEDGMENTS

The authors would like to thank Seppe Staelens for teaching and tutoring the advanced concepts of astrophysics of high-density objects and relativity required to begin research and produce this research paper, and for providing feedback on drafts. Special thanks to Dr. Daniel Mayerson for helping, sharing, and explaining the workings of FOORT code and for his book, *Relativity: A Journey Through Warped Space and Time*, which was used to study the theory of general relativity. Lastly, thanks to the Cambridge Centre for International Research for helping organize and execute this endeavor. This project would not have been possible without their support and expertise.

https://doi.org/10.59720/24-074

Received: February 25, 2024
Accepted: June 16, 2024
Published: August 12, 2025

REFERENCES

1. Oppenheimer, J. R. and Snyder H. "On Continued Gravitational Contraction." *Physical Review*, vol. 56, no. 5, 1 Sept. 1939, pp. 455–459, https://doi.org/10.1103/physrev.56.455.
2. Penrose, R. "Black Holes." *Scientific American*, vol. 226, no. 5, 1972, pp. 38–47, https://doi.org/10.2307/24927336.
3. Nadeem, M. S., et al. "Gravitational Force between the Black Hole & Light Particle in AGN." *Journal of Modern Physics*, vol. 04, no. 11, 2013, pp. 1524–1529, https://doi.org/10.4236/jmp.2013.411186.
4. Dubey, A. K., and Sen, A. K. "Frame-Dragging from Charged Rotating Body." *Journal of Physics Conference Series*, vol. 759, Oct. 2016, p. 012065, https://doi.org/10.1088/1742-6596/759/1/012065.
5. Bailyn, C. D. *What Does a Black Hole Look Like?* Princeton University Press, 2014, pp. 135–149, https://doi.org/10.2307/j.ctt6wq0ft.
6. Bolton, C. T. "Identification of Cygnus X-1 with HDE 226868." *Nature*, vol. 235, no. 5336, Feb. 1972, pp. 271–273, https://doi.org/10.1038/235271b0.
7. Miller-Jones, J. C. A., et al. "Cygnus X-1 Contains a 21–Solar Mass Black Hole—Implications for Massive Star Winds." *Science*, vol. 371, no. 6533, 18 Feb. 2021, pp. 1049-1049, https://doi.org/10.1126/science.abb3363.
8. Akiyama, K., et al. "First M87 Event Horizon Telescope Results. VII. Polarization of the Ring." *The Astrophysical Journal Letters*, vol. 910, no. 1, 1 Mar. 2021, p. L12, https://doi.org/10.3847/2041-8213/abe71d.
9. Narayan, R., and Eliot, Q. "Black Hole Accretion." *Science*, vol. 307, no. 5706, 2005, pp. 77–80, https://doi.org/10.2307/3839937.
10. Nightingale, J. W., et al. "Abell 1201: Detection of an Ultramassive Black Hole in a Strong Gravitational Lens." *Monthly Notices of the Royal Astronomical Society*, vol. 521, no. 3, Mar. 2023, pp. 3298–322, https://doi.org/10.1093/mnras/stad587.
11. Vegetti, S., et al. "Gravitational Detection of a Low-Mass Dark Satellite Galaxy at Cosmological Distance." *Nature*, vol. 481, no. 7381, Jan. 2012, pp. 341–43, https://doi.org/10.1038/nature10669.
12. Blinder, S. M. "Centennial of General Relativity (1915-2015); the Schwarzschild Solution and Black Holes." *ArXiv*, Jan. 2015, https://doi.org/10.48550/arxiv.1512.02061.
13. Kogut, John B. Special Relativity, Electrodynamics, and General Relativity: From Newton to Einstein. London, United States, Academic Press, 2018, pp. 285–300.
14. Perry, G. P. and Mann R. B. "Traversible Wormholes in (2 + 1) Dimensions." *General Relativity and Gravitation*, vol. 24, no. 3, Mar. 1992, pp. 305–21, https://doi.org/10.1007/bf00760232.
15. Lemos, J. P. S., et al. "Morris-Thorne Wormholes with a Cosmological Constant." *Physical Review D*, vol. 68, no. 6, 5 Sept. 2003, p. 064004, https://doi.org/10.1103/physrevd.68.064004.
16. Nandi, K. K., et al. "Gravitational Lensing by Wormholes." *Physical Review D*, vol. 74, no. 2, July 2006, p. 024020, https://doi.org/10.1103/physrevd.74.024020.
17. Perlick, V. "Exact Gravitational Lens Equation in Spherically Symmetric and Static Spacetimes." *Physical Review D*, vol. 69, no. 6, Mar. 2004, p. 064017, https://doi.org/10.1103/physrevd.69.064017.
18. Jeffers, J., and Reinders, J. *High Performance Parallelism Pearls*. 28 July 2015, pp. 349–358.
19. Staelens, S., et al. "Black Hole Photon Rings beyond General Relativity." *Physical Review*, vol. 107, no. 12, June 2023, p. 124026, https://doi.org/10.1103/physrevd.107.124026.
20. Tsukamoto, N., et al. "Can We Distinguish between Black Holes and Wormholes by Their Einstein-Ring Systems?" *Physical Review D*, vol. 86, no. 10, Nov. 2012, p. 104062, https://doi.org/10.1103/physrevd.86.104062.
21. Hu, Z., et al. "QED Effect on a Black Hole Shadow." *Physical Review. D.*, vol. 103, no. 4, 25 Feb. 2021, p. 044057 https://doi.org/10.1103/physrevd.103.044057.
22. Vincent, F. H., et al. "GYOTO: A New General Relativistic Ray-Tracing Code." *Classical and Quantum Gravity*, vol. 28, no. 22, Oct. 2011, p. 225011, https://doi.org/10.1088/0264-9381/28/22/225011.
23. Mitchell, J. S. B., et al. "The Discrete Geodesic Problem." *SIAM Journal on Computing*, vol. 16, no. 4, Aug. 1987, pp. 647–668, https://doi.org/10.1137/0216045.
24. "FOORT.sln." GitHub, ConfigReader, Mayerson D. and Bacchini F., 2023, https://github.com/drmayerson/FOORT/blob/ConfigReader/FOORT.sln
25. Weingard, R. "Some Philosophical Aspects of Black Holes." *Synthese*, vol. 42, no. 1, 1979, pp. 191–219, https://doi.org/10.2307/20115475.
26. Howard, S. "Black Holes Can Dance." *Journal of the Washington Academy of Sciences*, vol. 97, no. 2, 2011, pp. 1–28, www.jstor.org/stable/24536519.
27. Müller, T. "Einstein Rings as a Tool for Estimating Distances and the Mass of a Schwarzschild Black Hole." *Physical Review*, vol. 77, no. 12, 26 June 2008, p. 124042, https://doi.org/10.1103/physrevd.77.124042.
28. Lightman, A. P., et al. *Problem Book in Relativity and Gravitation*. Princeton University Press, 2017, pp. 87–91, https://doi.org/10.2307/j.ctvc774vf.19.
29. Shahar H. "Spherical Null Geodesics of Rotating Kerr Black Holes." *Physics Letters B*, vol. 718, no. 4-5, 1 Jan. 2013, pp. 1552–1556, https://doi.org/10.1016/j.physletb.2012.12.047.
30. Eyasmin, S., et al. "Curvature Properties of Morris-Thorne Wormhole Metric." *Journal of Geometry and Physics*, vol. 174, Apr. 2022, p. 104457, https://doi.org/10.1016/j.geomphys.2022.104457.